Carderock Division
Naval Surface Warfare Center
Bethesda, Maryland 20084–5000

NSWCCD-SIG-96/120-7030 October 1996
Signatures Directorate
Research and Development Report

Phenomenon of Leaky Free Waves in the Modal Response of a Uniform Cylinder

by

G. Maidanik
K.J. Becker

NSWCCD-SIG-96/120-7030 Phenomena of Leaky Free Waves in the Modal Response of a Uniform Cylinder

UNCLASSIFIED

SECURITY CLASSIFICATION OF THIS PAGE

REPORT DOCUMENTATION PAGE

Form Approved OMB No. 0704-0188

1a. REPORT SECURITY CLASSIFICATION Unclassified	1b. RESTRICTIVE MARKINGS None
2a. SECURITY CLASSIFICATION AUTHORITY	3. DISTRIBUTION / AVAILABILITY OF REPORT Approved for public release.
2b. DECLASSIFICATION/DOWNGRADING SCHEDULE	Distribution is unlimited.
4. PERFORMING ORGANIZATION REPORT NUMBER(S) NSWCCD-SIG-96/120-7030	5. MONITORING ORGANIZATION REPORT NUMBER(S)
6a. NAME OF PERFORMING ORGANIZATION NSWC, Carderock Division 6b. OFFICE SYMBOL *(If applicable)* Code 7030	7a. NAME OF MONITORING ORGANIZATION
6c. ADDRESS *(City, State, and ZIP Code)* Bethesda, MD 20084-5000	7b. ADDRESS *(City, State, and ZIP Code)*
8a. NAME OF FUNDING/SPONSORING ORGANIZATION 8b. OFFICE SYMBOL *(If applicable)*	9. PROCUREMENT INSTRUMENT IDENTIFICATION NUMBER
8c. ADDRESS *(City, State, and ZIP Code)*	10. SOURCE OF FUNDING NUMBERS PROGRAM ELEMENT NO. / PROJECT NO. / TASK NO. / WORK UNIT ACCESSION NO.

11. TITLE *(Include Security Classification)*
Phenomenon of Leaky Free Waves in the Modal Response of a Uniform Cylinder

12. PERSONAL AUTHOR(S)
G. Maidanik and K.J. Becker

13a. TYPE OF REPORT	13b. TIME COVERED	14. DATE OF REPORT *(Year, Month, Day)*	15. PAGE COUNT
Research & Development	FROM 960101 TO 961031	1996 October 31	31

16. SUPPLEMENTARY NOTATION

17. COSATI CODES			18. SUBJECT TERMS *(Continue on reverse if necessary and identify by block number)*
FIELD	GROUP	SUB-GROUP	Structural Acoustics Leaky Free Waves Wave Propagations

19. ABSTRACT *(Continue on reverse if necessary and identify by block number)*

The phenomenon of leaky free waves in the modal response of a uniform shell is manifest if (1) in the absence of fluid loading the locus of the free waves as a function of frequency crosses from the subsonic region to the supersonic region across the sonic locus and (2) in the presence of fluid loading the fluid surface impedance at and in the vicinity of the sonic locus is high and the introduction of this fluid loading does not prevent the free waves of concern from reaching the sonic locus. The phenomenon of leaky free waves in the modal response of a uniform cylinder is investigated. It is found that two distinct examples of leaky free waves are manifested. The first is associated with the flexural free waves that reside in a frequency range that lies above the critical frequency with respect to the speed of sound in the fluid and the second is associated with the curvature free waves that reside in a frequency range that lies below the ring frequency. The phenomenon of leaky free waves in these two examples is computed, displayed and discussed.

20. DISTRIBUTION / AVAILABILITY OF ABSTRACT	21. ABSTRACT SECURITY CLASSIFICATION
☒ UNCLASSIFIED/UNLIMITED ☐ SAME AS RPT. ☐ DTIC USERS	Unclassified
22a. NAME OF RESPONSIBLE INDIVIDUAL Maidanik, G.	22b. TELEPHONE *(Include Area Code)* (301)227-1292 22c. OFFICE SYMBOL NSWCCD 7030

DD Form 1473, JUN 86 *Previous editions are obsolete.*

SECURITY CLASSIFICATION OF THIS PAGE

UNCLASSIFIED

CONTENTS

ABSTRACT

The phenomenon of leaky free waves in the modal response of a uniform shell is manifest if (1) in the absence of fluid loading the locus of the free waves as a function of frequency crosses from the subsonic region to the supersonic region across the sonic locus and (2) in the presence of fluid loading the fluid surface impedance at and in the vicinity of the sonic locus is high and the introduction of this fluid loading does not, in itself, prevent the free waves of concern from reaching the sonic locus. In this consideration the sonic locus remains fixed relative to the properties of the shell and, therefore, changes in the fluid loading, on a given shell, are induced by changes in the fluid density only. The phenomenon of leaky free waves in the modal response of a uniform cylinder is investigated. It is found that two distinct examples of leaky free waves are manifested. The first is associated with the flexural free waves that reside in a frequency range that lies above the critical frequency with respect to the speed of sound in the fluid and the second is associated with the curvature free waves that reside in a frequency range that lies below the ring frequency. The phenomenon of leaky free waves in these two examples is computed, displayed and discussed.

INTRODUCTION

In a recent report and a recent paper the authors dealt with the analysis of the normalized modal response $\overline{V}_n(k,\omega)$ of **hybrid** and **natural** fluid loaded cylinders subjected to a normalized modal external drive $\bar{P}_{en}(k,\omega)$, where, (k) is the axial wavenumber variable, (ω) is the frequency variable and (n) is the circumference mode index [1,2]. Section II of Reference 2 is to be considered an integral part of this introduction. In particular, Eqs. (1) through (15) in Section II of Reference 2 now become Eqs. (1) through (15) in the present report. In this section the investigation is limited to situations for which $(\omega_r / \omega_c) << 1$, to the lower mode indices, $n \lesssim 9$; and to the spectral range $\{0, (2\omega_r / \omega_c)\} \lesssim \{(ak), (\omega / \omega_c)\} \lesssim \{75, 0.6\}$, where (a) is the radius of the cylinder, (ω_r) is the ring frequency and (ω_c) is the critical frequency of the flexural free waves with respect to the speed of sound (c). [In this report, as in Reference 2, the ratio, of the speed of sound (c) to the longitudinal speed (c_ℓ) in the plating of the cylinder, remains fixed. Therefore, changes in the characteristic impedance of the fluid on a cylinder with specific material properties, are induced by changes in the fluid density (ρ) only.] As much as this spectral range is of interest, there is a compelling investigative interest to extrapolate the range at both extremities. Of chief concern in this report is the extrapolation that involves the phenomenon of "leaky free waves". As can be inferred, here the phenomenon of leaky free waves is manifest and investigated in the normalized spectral domain; namely, either in the $\{(ak), (\omega / \omega_c)\}$−domain or in the $\{(ak), (\omega / \omega_r)\}$−domain [3]. Since this phenomenon with respect to the "flexural free waves" at the higher frequency range, where $(\omega / \omega_c) \gtrsim 1.0$, is reasonably familiar, whereas this phenomena with respect to the "membrane free waves" at the lower frequency range, where $(\omega / \omega_r) \lesssim 2.0$, is hardly familiar, the story in this report begins with the extrapolation of the investigation into the higher frequency range just defined [3-5]. Under the conditions that $(\omega_r / \omega_c) << 1$ and $n \lesssim 9$, the phenomenon of leaky flexural free waves occurs in the

partial response of a panel, and the modal responses of a hybrid cylinder and a natural cylinder [1]. Indeed, the literature deals with this phenomenon in all three of these shells [3-5]. Moreover, the differences in this phenomenon with a specific shell form are negligible; once it is accounted for in one shell, it is well nigh accounted for in any of the others [6]. On the other hand, it is recognized that neither the panel nor the hybrid cylinder exhibit membrane free waves and, therefore, only a natural cylinder is relevant to investigating the phenomenon of leaky free waves at the lower frequency range, where $(\omega/\omega_r) \lesssim 2.0$ [1,2]. In addition, the present report deals with uniform shells only; ribbed shells are dealt with in a companion report that follows.

Accepting that "familiarity breeds contempt," the leaky flexural free waves phenomenon at the higher frequency range, where $(\omega/\omega_c) \gtrsim 1.0$, is briefly repeated here so that the subsequent comparison with the leaky membrane free waves phenomenon at the lower frequency range, where $(\omega/\omega_r) \lesssim 2.0$, can be facilitated.

At this early stage a word or two about the figures presented in this report may be useful. Typically, the figures depict the normalized quantity $|\overline{S}(k,\omega)|$ "as a function of (ak) in a frequency waterfall format [7]." This quantity is displayed in terms of the quantity $\overline{S}'_q(ak)$ as a function of (ak). These quantities are related in the manner

$$\overline{S}'_q(ak) = \log [|\overline{S}\{k,\omega_o+(q+1)\Delta\omega\}|10^q] = q+\log |\overline{S}\{k,\omega_o+(q+1)\Delta\omega\}|,$$

where (ω_o) is the frequency lower bound; $\omega_o \lesssim \omega$, $(\Delta\omega)$ is an incremental frequency band and (q) is an integer bounded by $0 \leq q \leq q_f$. As stated in the figure captions in this report, the $\overline{S}(k,\omega)$, in $\overline{S}'_q(ak)$, is the normalized modal response $\overline{V}_{\infty n}(k,\omega)$. This equation states that the frequency is identified on the step-wise frequency axis by the frequency pseudonym 10^q, which locates the origin of the curve pertaining to the normalized frequency $(\omega/\omega_c) = [(\omega_o/\omega_c) + (q+1)\ \Delta(\omega/\omega_c)]$. It follows that the number of curves in a figure is equal to the "upper bound integer" (q_f) plus one and that

(ω_c) is merely a convenient normalizing frequency. The spectral range for a display is defined by

$$\{(ak_o),\ (\omega_o/\omega_c)\} \lesssim \{(ak),\ (\omega/\omega_c)\} \lesssim \{(ak_f),\ (\omega_f/\omega_c)\}\ ,$$

yielding an estimate of q_f in the form $[(\omega_f/\omega_c) - (\omega_o/\omega_c)] \approx (q_f+1)\ \Delta\ (\omega/\omega_c)$. For example, from Fig. 1a it is deduced that $60 < q_f < 70$; indeed, in this figure $(\omega_o/\omega_c) = 0.47$, $q_f = 65$ and $\Delta(\omega/\omega_c) = 0.03$, where the normalizing frequency (ω_c) is identified to be the critical frequency of the flexural free waves. Analogously, from Fig. 6a it is deduced that $98 < q_f < 103$; indeed, in this figure $(\omega_o/\omega_r) = 0$, $q_f = 101$ and $\Delta(\omega/\omega_r) = 0.014$, where the normalizing frequency (ω_r) is identified to be the ring frequency of the cylinder. Siltuations arise in which a feature in a display may be accentuated were the number of the displayed curves made more sparse; e.g., by successively displaying only one out of a fixed number of curves. This specific procedure is used in this report; e.g., in Fig. 1a every other curve is omitted and, therefore, only 33 out of 66 curves are shown. Analogously, in Fig. 6a two curves out of three are omitted and, therefore, only 34 out of 102 curves are shown. Other variations on the display theme may be similarly defined and introduced when one or another feature calls. The sonic locus positions in the figures are determined, in the context of the report, in the compatible form

$$(ak)^2 = [\{(\omega_o/\omega_c) + (q+1)\ \Delta(\omega/\omega_c)\}^2 (ak_c)^2 - n^2]; \quad k_c = (\omega_c/c)\ ,$$

where, again, (ω_c) is merely a convenient normalizing frequency and (q) is the integer just defined with respect to the frequency waterfall format.

I. PHENOMENON OF LEAKY FLEXURAL FREE WAVES IN A FLUID LOADED UNIFORM CYLINDER

From Eq. (13a) the absolute value of the normalized modal response $|\overline{V}_{\infty n}(k,\omega)|$ [$\equiv |\overline{G}_{\infty n}(k,\omega)|$] is evaluated as a function of (ak) in a frequency waterfall format [1,7]. The evaluation in this section is a "zoom on" the higher spectral range in which the critical frequency is approached and surpassed. This spectral range starts at the upper limits of the range previously considered in Reference 2 and extends the normalized frequency range to an octave above the critical frequency; the zoom on in the higher spectral range is thus defined: $\{70,\ 0.5\} \lesssim \{(ak),\ (\omega/\omega_c)\} \lesssim \{150,\ 2.5\}$. [As already mentioned, in this range the partial (or modal) response is substantially invariant to the form of the shell.] The phenomenon of leakage of free waves is advantageously introduced via a situation in which it is absent; a situation of light fluid loading. Note that a moderate fluid loading is characterized by the standard fluid loading parameter $\varepsilon_c = 10^{-2}$, a light fluid loading is characterized by $\varepsilon_c \lesssim 10^{-4}$ and a heavy fluid loading by $\varepsilon_c \gtrsim 10^{-1}$. Also note that the change in the fluid loading parameter, in the context of this report, is effected by the fluid density (ρ); the fluid speed of sound (c) remains unchanged. Figures 1a through c depict $\overline{V}_{\infty n}(k,\omega)$, as a function of (ak) in a frequency waterfall format, in the higher spectral range just defined, for three values of the mode index; $n = 0,\ 1$ and 9, respectively and for light fluid loading; $\varepsilon_c = 10^{-4}$. The sonic locus is superimposed on these figures so that its location can be identified. The flexural locus, constituted by the ridges and associated peaks, defines the flexural free waves in these figures. Clearly, as the normalized frequency increases from $(\omega/\omega_c) = 0.5$, the flexural locus converges on the sonic locus from the subsonic region. When (ω/ω_c) reaches unity, this convergence is completed. As (ω/ω_c) is increased beyond unity, the flexural locus crosses the sonic locus unimpeded and begins to diverge from it into the supersonic

region. The flexural locus diverges more and more from the sonic locus as (ω/ω_c) further increases on to two (2) and beyond.

Figures 2a through c repeat Figs. 1a through c, respectively, except that the standard fluid loading parameter is restored; $\varepsilon_c = 10^{-2}$. The sonic locus, defining a spectral region of high fluid surface impedance, is discernible in these figures. Even for this moderate fluid loading, the fluid surface impedance is high enough to imprint the sonic locus on these figures. This high fluid surface impedance at the sonic locus establishes a barrier which impedes the crossing of the flexural free waves from the subsonic region into the supersonic region. As the normalized frequency (ω/ω_c) increases past unity, the flexural locus is held at bay adjacent to the barrier on the subsonic side. As the normalized frequency is further increased, however, a gradual commencement of leakage of flexural free waves through the barrier at the sonic locus into their rightful place in the supersonic region, occurs. The leakage is substantially completed when (ω/ω_c) is two (2).

The higher fluid loading, that is essential to the manifestation of the phenomenon of leaky flexural free waves, introduces an additional phenomenon. Clearly, the flexural free waves that are in the supersonic region are efficient radiators compared with those in the subsonic region. When fluid loading is light, this difference is not significant since radiation damping, even for the supersonic-flexural free waves, is not high enough to compete with the inherent mechanical damping. However, when fluid loading is moderate, the radiation damping of the supersonic flexural free waves becomes significant, as can be verified by comparing Figs. 1 and 2.

Figures 3a1, b and c repeat Figs. 2a through c, respectively, except that the fluid loading parameter is changed from the moderate standard value of 10^{-2} to the high value of 10^{-1}. Comparing Figs. 3a1, b and c and 2a through c, respectively, shows the increased effectiveness of the fluid loading barrier in the former set of figures and the accompanied decrease in the leakage of flexural free waves across this barrier. The more gradual

leakage across the more effective barrier results in a wider frequency band to complete the leakage. Thus, this frequency band in Figs. 3a1, b and c is wider than in Figs. 2a through c, respectively. Indeed, the completion of the leakage in Figs. 3a1, b and c takes place beyond the frequency range used for these figures, as Fig. 3a2 attests. Moreover, as expected, the radiation damping of the flexural free waves, in the supersonic region, is higher in Figs. 3a1, b and c than in Figs. 2a through c, respectively.

The phenomenon of leaky free waves is thus predicated on the existence of free waves that, in the absence of fluid loading, transit, as a function of frequency, across the sonic locus. In addition, the fluid loading needs to be high enough to establish an effective barrier that substantially impedes this crossing. The flexural free waves in a panel, in a hybrid cylinder and in a natural cylinder satisfy the first of these requirements. Are there other types of free waves on a shell that similarly satisfy this first requirement? The natural cylinder is the only shell of these mentioned that needs to be examined in light of this question; the other two shells support, by definition, flexural free waves only, whereas the natural cylinder supports, in addition, membrane free waves.

II. BEHAVIOR IN THE LOWER FREQUENCY RANGE OF THE MEMBRANE FREE WAVES IN A NATURAL UNIFORM CYLINDER

Again, advantageously the phenomenon of leakage in the membrane free waves is introduced via a situation in which it is absent; a situation of light fluid loading. From Eq. (13a) the absolute value of the normalized modal response $|\overline{V}_{\infty n}(k,\omega)| = [\equiv|\overline{G}_{\infty n}(k,\omega)|]$ is evaluated as a function of (ak) in a frequency waterfall format [1,7]. This evaluation is confined to the lower spectral range defined by $\{0,0\} \lesssim \{(ak), (\omega/\omega_r)\} \lesssim \{25, 2.4\}$. The modal response, pertaining to the membrane free wave, is more characteristically identified in a frequency waterfall representation that employs a frequency normalization by the ring frequency (ω_r), rather than by the critical frequency (ω_c). Figures 4a and b1 and 5a and b1 are evaluated under standard parametric values except that the fluid loading parameter (ε_c) is changed from the standard value of 10^{-2} to 10^{-4} and in the first set of figures the mode index (n) is zero and in the second the standard value of unity prevails. Figures 4a and 5a pertain to a hybrid cylinder and the corresponding Figs. 4b1, and 5b1 pertain to a natural cylinder. Comparing Figs 4a and 5a with Figs. 4b1 and 5b1, respectively, shows that the membrane free waves are composed of longitudinal and curvature free waves in Fig. 4b1 and of longitudinal, shear and curvature free waves in Fig. 5b1.

Figure 4b1, for which the mode index (n) is equal to zero, exhibits the birth of the longitudinal free waves at $\{(ak), (\omega/\omega_r)\} \simeq \{0, 1.0\}$. In the normalized frequency range below unity $(\omega/\omega_r) \lesssim 1$, the longitudinal locus is absent. Close to its spectral place of birth, the speed of the longitudinal free waves is high, decreasing rapidly and converging on to the longitudinal speed (c_ℓ) as the normalized frequency (ω/ω_c) increases past unity; the longitudinal speed (c_ℓ) is independent of frequency. On the outside and adjacent to the longitudinal locus lies an "anti-longitudinal locus" that is defined by valleys and associated nadirs. This anti-longitudinal locus maintains the longitudinal speed and it continues uninterrupted as the normalized frequency (ω/ω_r) is

decreased below unity and on to the spectral origin at $\{(ak),\ (\omega/\omega_r)\} = \{0,0\}$. Again, there are no shear and anti-shear loci patterns for $n=0$ [1]. Finally, the flexural free waves at the lower frequency range, where $(\omega/\omega_r) \lesssim 2.0$, are superseded by curvature free waves. The speed of the curvature free waves surpasses that of the corresponding flexural free waves more and more as (ω/ω_r) decreases below two (2) and on to unity [cf. Fig. 4a.]. As (ω/ω_r) decreases further below unity, the speed of the curvature locus, that defines the curvature free waves, assumes the longitudinal speed, positioning itself on the outside of and adjacent to the anti-longitudinal locus. The curvature free waves in that position are guided by the anti-longitudinal locus all the way to the spectral origin. Since the longitudinal speed (c_ℓ) is higher than the speed of sound (c), as defined in Eq. (15), the curvature free waves emerge as a potential candidate to exhibit the phenomenon of leaky free waves. Confluently, this description designates (ω_r) to be the "critical frequency", with respect to the speed of sound (c), of the curvature free waves pertaining to the zeroth mode index [2].

Figure 5b1, for which the mode index (n) is equal to the standard value of unity, exhibits both the longitudinal locus and the shear locus [1]. Moreover, each is accompanied on the outside by an adjacent anti-locus; an anti-longitudinal locus and an anti-shear locus. In Fig. 5b1 neither of these loci nor the accompanying anti-loci extend beyond $(\omega/\omega_r) \simeq (1/2)$; the birth of the longitudinal locus is at a higher normalized frequency than in Fig. 4b1 and the birth of the shear locus in Fig. 5b1 is at $(\omega/\omega_r) \simeq (1/2)$. The longitudinal and anti-longitudinal loci asymptotically approach the longitudinal speed (c_ℓ) and the shear and anti-shear loci asymptotically approach the shear speed (c_s); none of these loci cross or even closely approach the sonic locus and, therefore, none is a potential candidate to generate leaky free waves. On the other hand, again at the lower frequency range, where $(\omega/\omega_r) \lesssim 2.0$, the flexural free waves are superseded by curvature free waves. The speed of the curvature free waves surpasses that of the corresponding flexural free waves more and more as (ω/ω_r) decreases below

(2) and on to unity. [cf. Fig. 5a.] As (ω/ω_r) decreases further below unity, the speed of the curvature locus become more and more independent of frequency as it makes its way toward the spectral origin at $\{(ak),\ (\omega/\omega_r)\} \cong \{0,0\}$. In Fig. 5b1 this asymptotic speed is approximately the shear speed (c_s), *ha*!, may be a shade lower. In addition, the off-set in the sonic locus when $n = 1$ helps render the curvature free waves in Fig. 5b1 only marginally a potential candidate to exhibit the phenomenon of leaky free waves.

Clearly, for a mode index (n) that exceeds unity, the curvature of the cylinder is even weaker than it is for a mode index of unity and, therefore, the conversion of the flexural free waves into curvature free waves is less effective. Under the parametric values specified in Eq. (15), which are central in the evaluations in this report, the phenomenon of leaky waves is not expected for mode indices that exceed unity, is only marginally expected for a mode index of unity, and is definitely expected for a mode index of zero.

III. PHENOMENON OF LEAKY CURVATURE FREE WAVES IN A FLUID LOADED NATURAL UNIFORM CYLINDER

A "zoom on region" where the phenomenon of leaky curvature free waves can be effectively and conveniently observed is, in the lower spectral range, defined by $\{0,0\} \lesssim \{(ak), (\omega/\omega_r) \lesssim \{4.0, 1.4\}$; this spectral range is sufficient to expose the essential features in the phenomenon. Figure 6a is the zoom on region taken out of Fig. 4b1; in these figures the mode index (n) is zero and the fluid loading parameter (ε_c) is light at 10^{-4}. In Fig. 6a, as in Fig. 4b1, the leaky free waves phenomenon is absent. Figure 6b repeats Fig. 6a except that the standard fluid loading parameter is restored; $\varepsilon_c = 10^{-2}$. Observe that in general the longitudinal free waves are substantially subdued by radiation damping that the fluid loading encourages; after all, the longitudinal locus lies in the supersonic spectral region. Moreover, the higher fluid loading in Fig. 6b, as compared with that in Fig 6a, tends to delay and mollify the transition of curvature free waves from the flexural free waves that they supersede. [cf. Appendix A.] As the normalized frequency (ω/ω_r) is decreased past unity, the curvature free waves are held at bay by the fluid loading barrier at the sonic locus. Further decrease in (ω/ω_r) introduces a gradual leakage of curvature free waves that gradually re-establishes the curvature locus at its rightful position adjacent and on the outside of the anti-longitudinal locus. [cf. Fig. 6a.] The leakage is complete when the normalized frequency (ω/ω_r) reaches the value of one third (1/3). [cf. Section I and, in particular, the comparison between Figs. 1a and 2a.] Figure 6c repeats Fig. 6b except that the standard fluid parameter is changed to the higher value of 10^{-1}. Compared with Fig. 6b, the features in Fig. 6c that are associated with the influences of fluid loading and, in particular, with the phenomenon of leaky curvature free waves, are more pronounced. Again, the normalized frequency band to complete the leakage is wider and extends further toward the spectral origin at $\{(ak),(\omega/\omega_r) = \{0,0\}$. [cf. compare Figs. 2 and 3.]

A zoom on region where the marginal phenomenon of leaky curvature free waves can be effectively and conveniently observed is in the same spectral range employed in Fig. 6. Figure 7a depicts the zoom on region taken out of Fig. 5b1; in these figures the mode index (n) is unity and the fluid loading parameter (ε_c) is light at 10^{-4}. In Fig. 7a, as in Fig. 5a, the leaky free wave phenomenon is absent even in a marginal form. Figure 7b repeats Fig. 7a except that the fluid loading parameter is restored to the standard value of 10^{-2}. Observe that in general the longitudinal and the shear free waves are substantially subdued by radiation damping that is caused by the increase in fluid loading; Eq. (15) dictates that both, the longitudinal and shear loci, lie in the supersonic spectral region; $c_\ell > c_s > c$. Moreover, the higher fluid loading and mode index in Fig. 7b, as compared with Figs. 7a and 6b, respectively, conspire to delay and mollify the transition of the curvature free waves from the flexural free waves that they supersede. As (ω/ω_r) is decreased past unity, the curvature free waves are held at bay by the fluid loading barrier at the sonic locus. [cf. Fig. 7a.] There is no true leakage, the curvature locus is merely held adjacent and on the subsonic side of the sonic locus all the way to the spectral origin. Figure 7c repeats Fig. 7b except that the standard fluid loading parameter is changed to the higher value of 10^{-1}. Again, compared with Fig. 7b, the features in Fig. 7c that are associated with the influences of fluid loading and, in particular, with the marginal phenomenon of leaky curvature free waves, are more pronounced. Indeed, the transition of the curvature free waves, from the flexural free waves that then supersede, is sufficiently delayed and mollified by the increased fluid loading that the phenomenon of leaky curvature free waves, in Fig 7c, is not even marginally manifested. [cf. Figs. 6b and c, and Appendix A.]

APPENDIX A

The mollifying effects of fluid loading on scattering and other structural response phenomena are well known [1,4,5]. It may then be helpful to briefly consider the role that fluid loading may play in the transition, as such, of flexural free waves into curvature free waves. Since this transition is more pronounced the lower the mode index is, only $n = 0$ and $n = 1$ are selected for the investigation in this appendix.

Figures 4b2 and 4b3 repeat Fig. 4b1 except that the fluid loading parameters (ε_c) is changed from 10^{-4} to the standard value of 10^{-2} and to the higher value of 10^{-1}, respectively. Disregarding the phenomenon of leaky curvature free waves that is discussed in the text, these three figures clearly show that increases in fluid loading tend to delay and mollify the transition to curvature free waves from the flexural free waves that they supersede [1,2]. These effects are only slight from Fig 4b1 to Fig. 4b2, but are substantial from Fig. 4b1 to Fig. 4b3. Nonetheless, even at the high value of 10^{-1} for the fluid parameter (ε_c), the delay and mollifying effects of fluid loading are not sufficient to scuttle the phenomenon of leaky curvature free waves, as Fig. 6c verifies.

Figures 5b2 and 5b3 repeat Fig. 5b1 except that the fluid loading parameter (ε_c) is changed from 10^{-4} to 10^{-2} and 10^{-1}, respectively. Again, disregarding the phenomenon of leaky curvature free waves that is discussed in the text, these three figures clearly show that increases in fluid loading tend to delay and mollify the transition to curvature free waves from the flexural free waves that they supersede [1,2]. Although these effects are only slight from Fig. 5b1 to Fig. 5b2, they are sufficient to render the curvature free waves subsonic, notwithstanding that at and in the vicinity of $(\omega / \omega_r) \simeq (1/2)$ the curvature free waves are only just subsonic. [cf. Fig. 7b.] On the other hand, the effects are substantial from Fig. 5b1 to Fig. 5b3. Indeed, the high fluid loading, in this case, renders the curvature free waves well nigh subsonic, as Fig. 7c verifies.

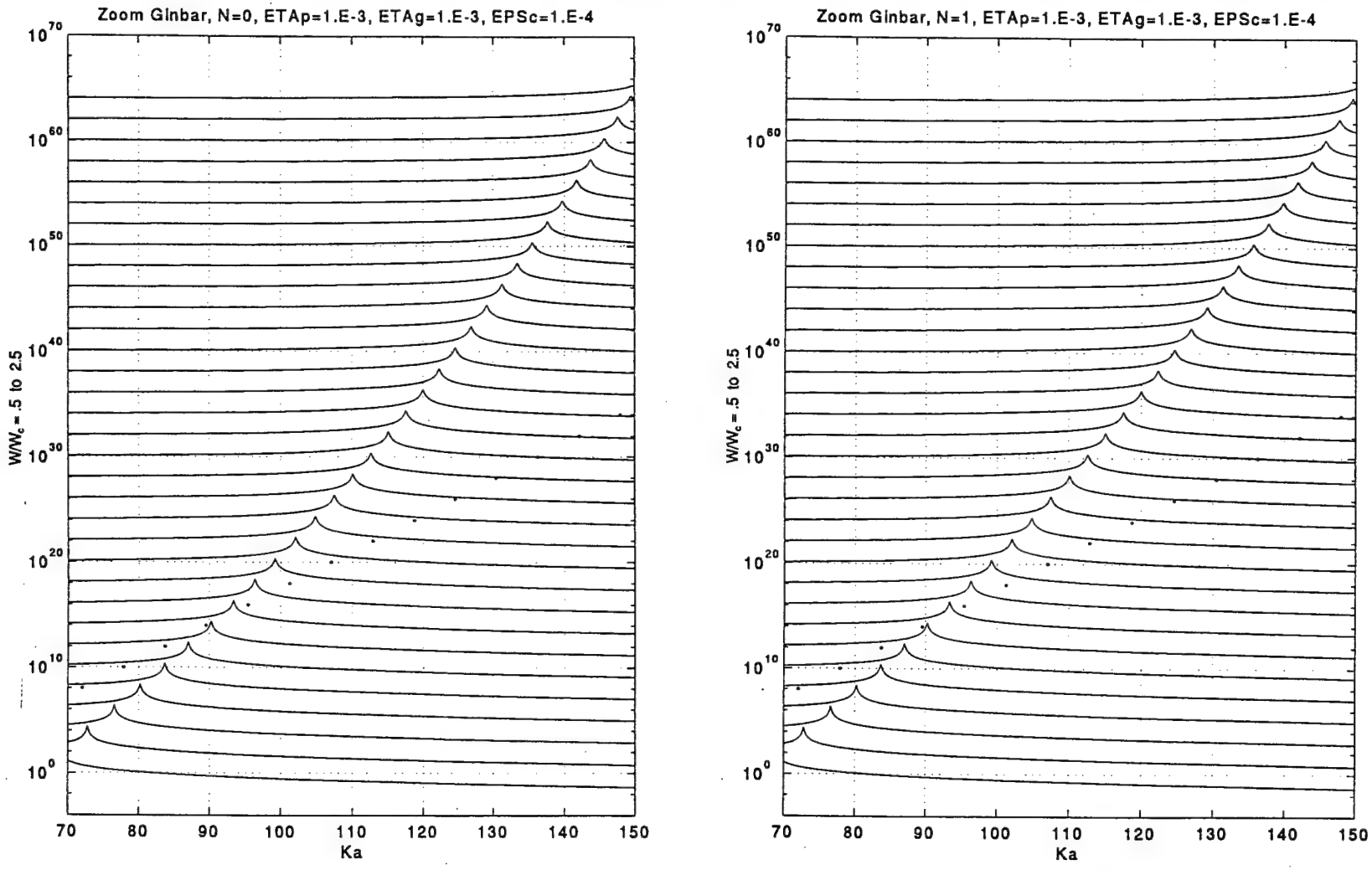

a. $n = 0$.

b. $n = 1$.

Fig. 1. The normalized modal response $\overline{V}_{\infty n}(k, \omega)$ as a function of (ak) in a frequency waterfall format pertaining to the higher spectral range. Standard parametric values are used, except that the fluid loading parameter (ε_c) is changed from the standard value of 10^{-2} to 10^{-4} and the mode index (n) is as specified. Superimposed is the sonic locus represented by discrete dots.

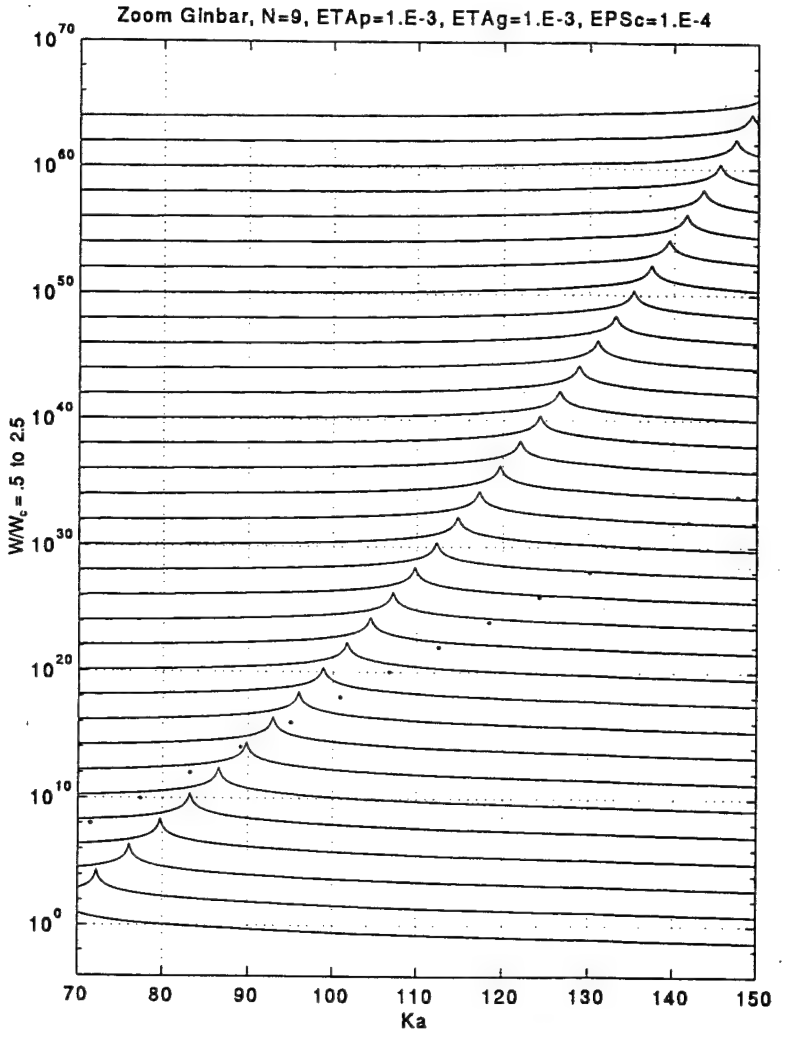

c. $n = 9$.

Fig. 1. Continued.

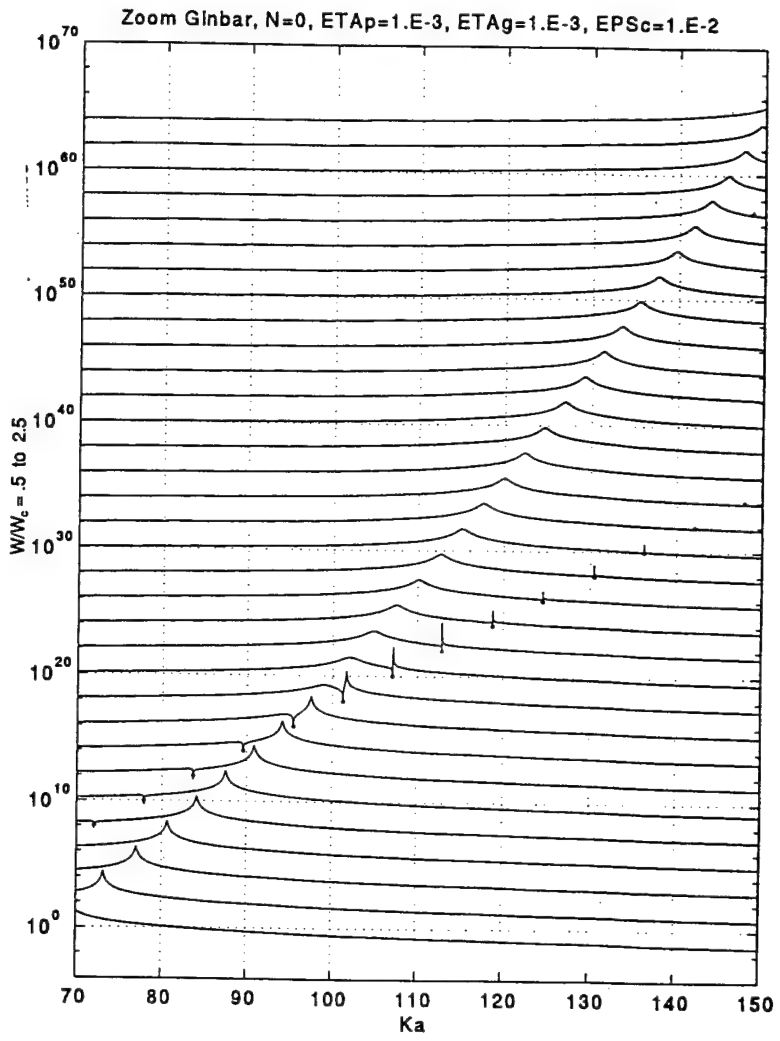

a. $n = 0$.

Fig. 2. As Fig. 1 except that the fluid loading parameter (ε_c) is restored to the standard value of 10^{-2}.

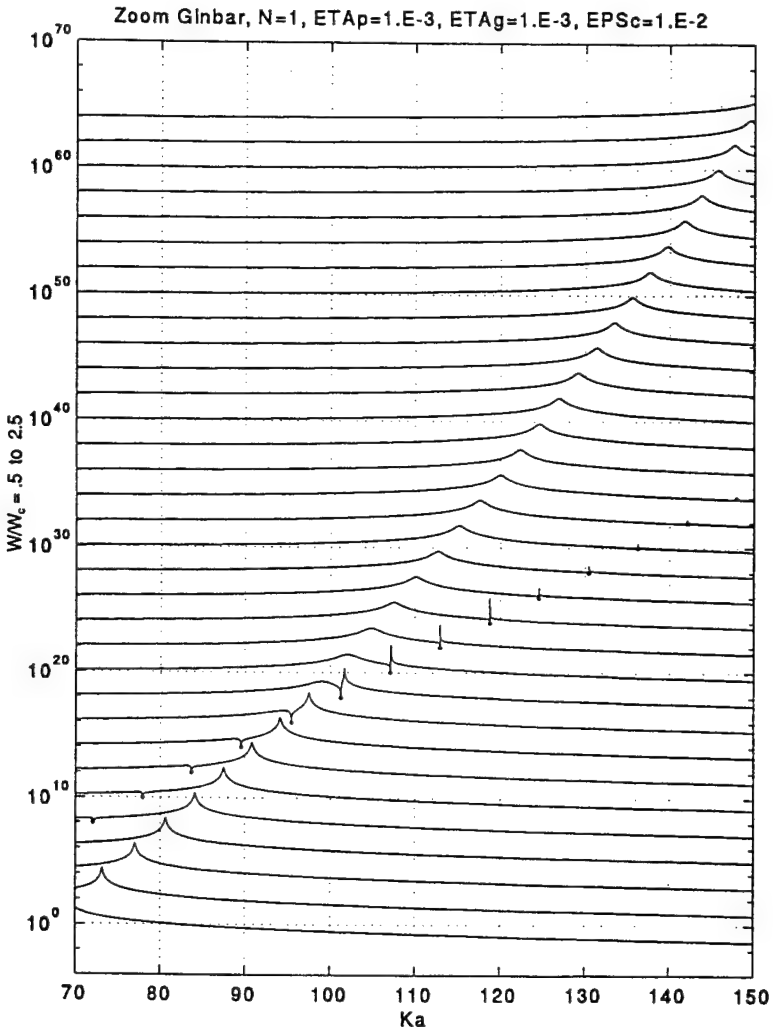

b. $n = 1$.

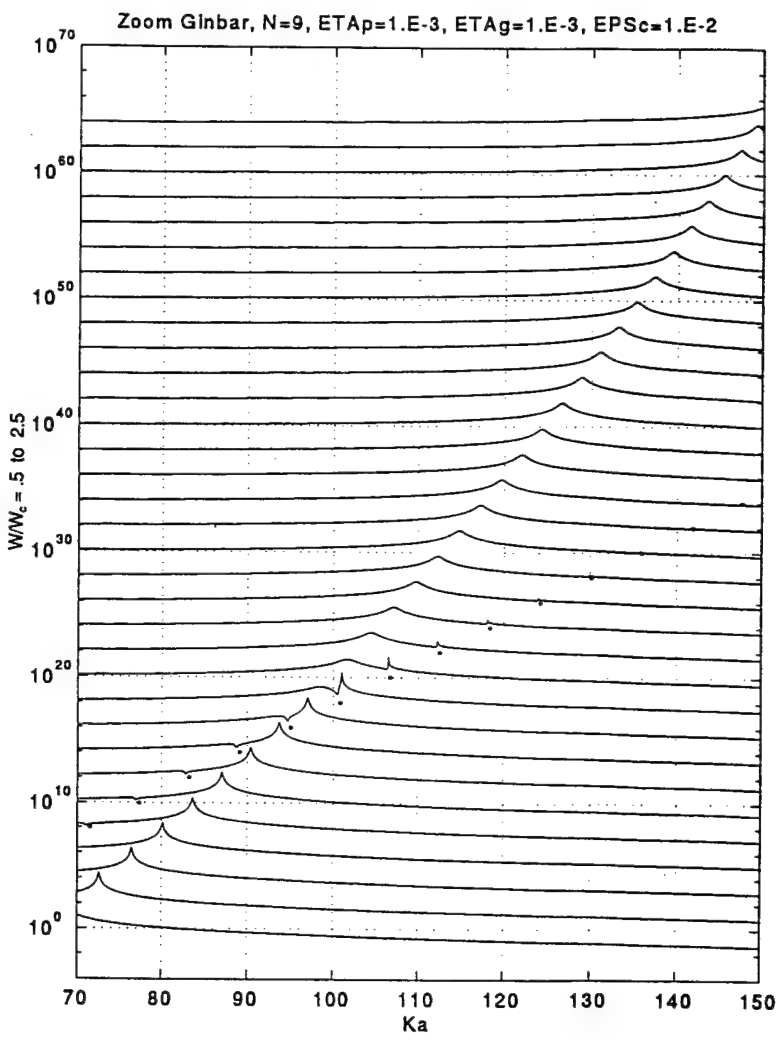

c. $n = 9$.

Fig. 2. Continued

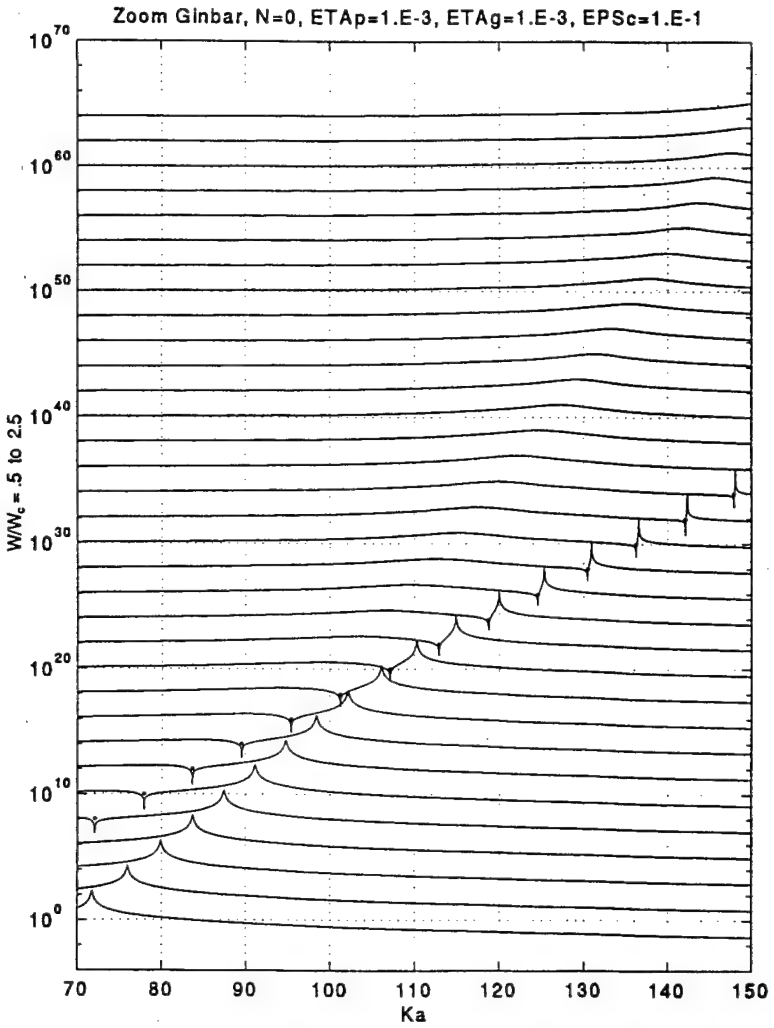

a1. $n = 0$.

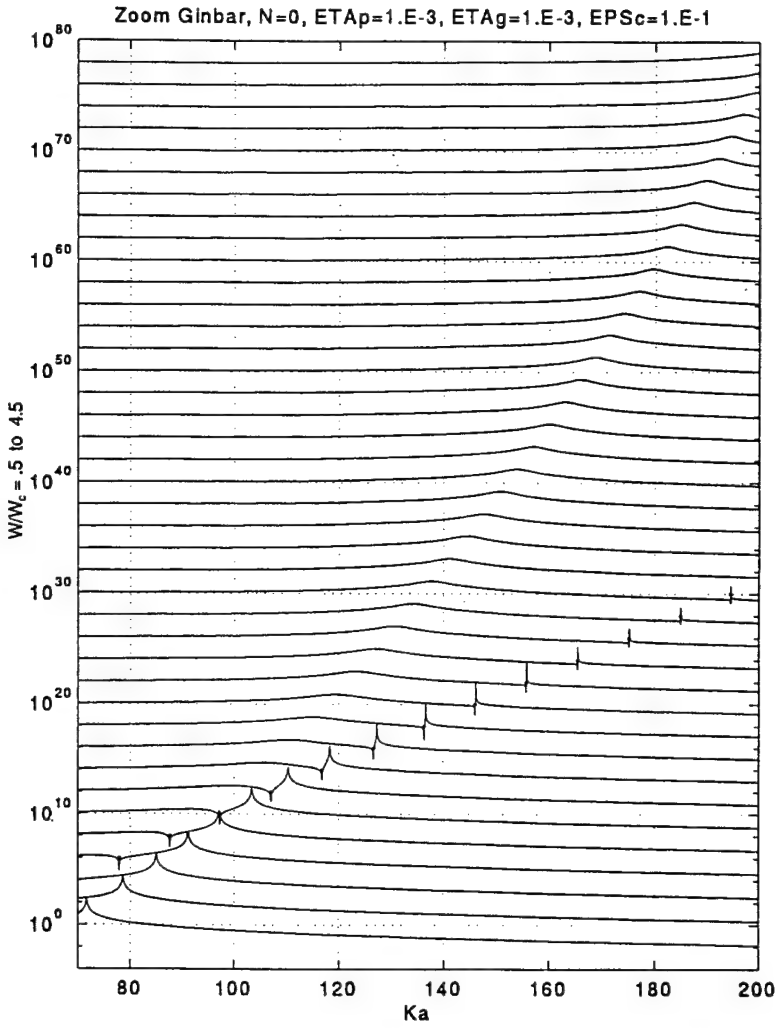

a2. As in Fig. 3a1 except that the spectral range is extended.

Fig. 3. As Fig. 1 except that the fluid loading parameter (ε_c) is changed from the value of 10^{-4} to 10^{-1}.

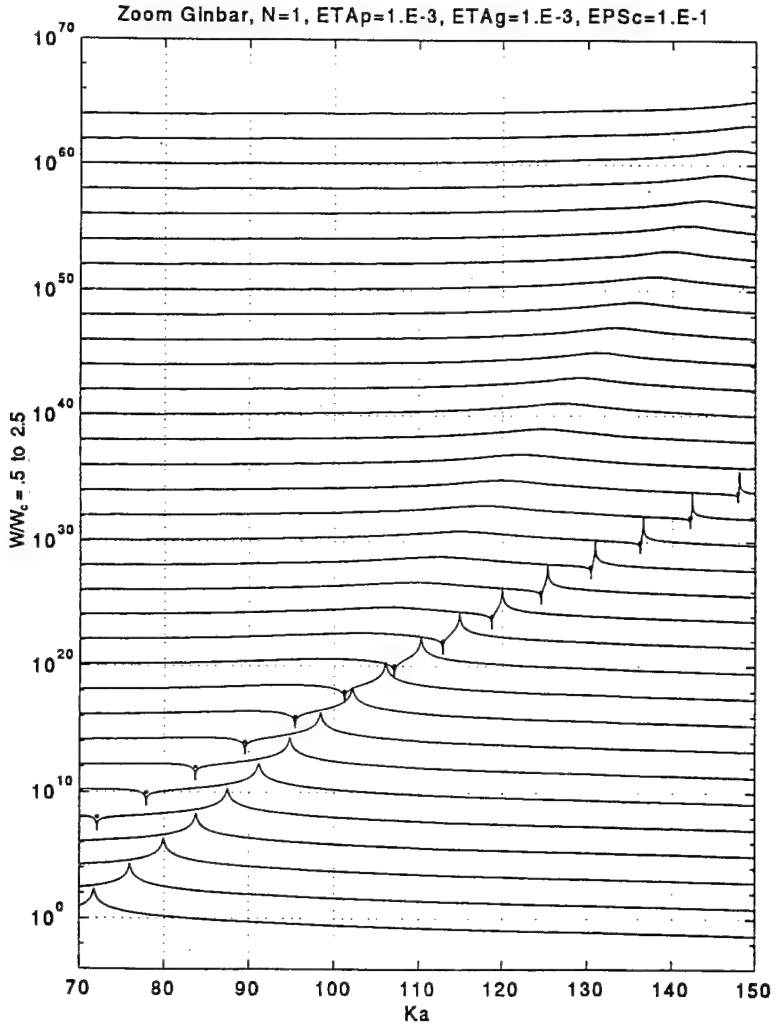

b. $n = 1$.

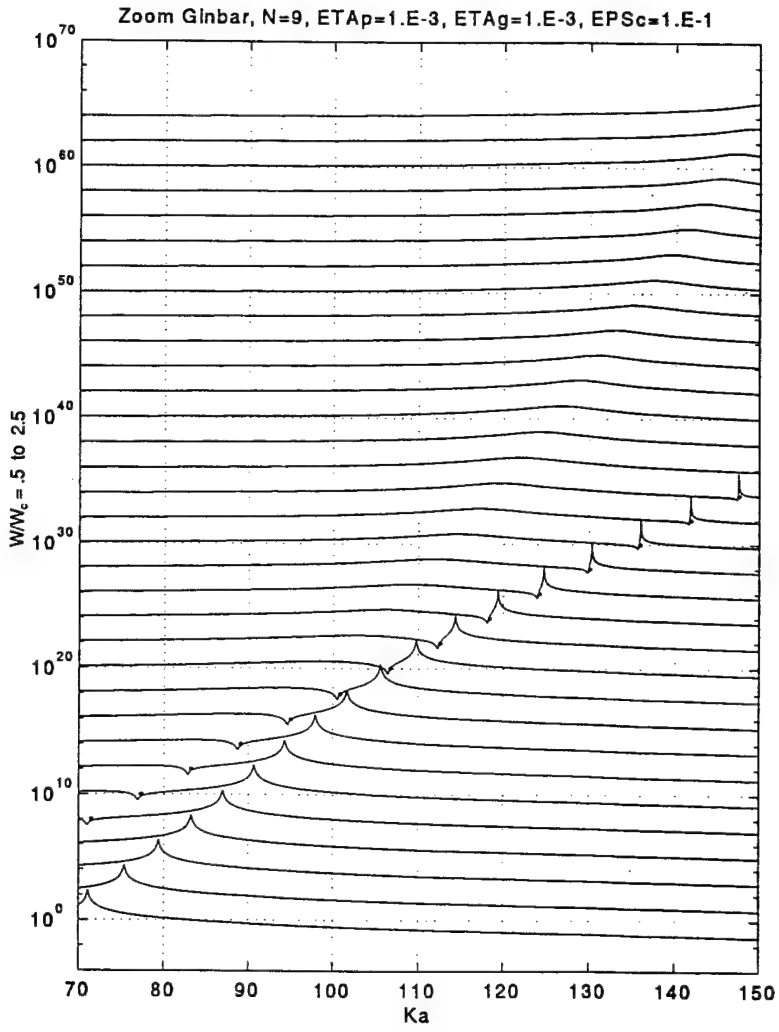

c. $n = 9$.

Fig. 3. Continued

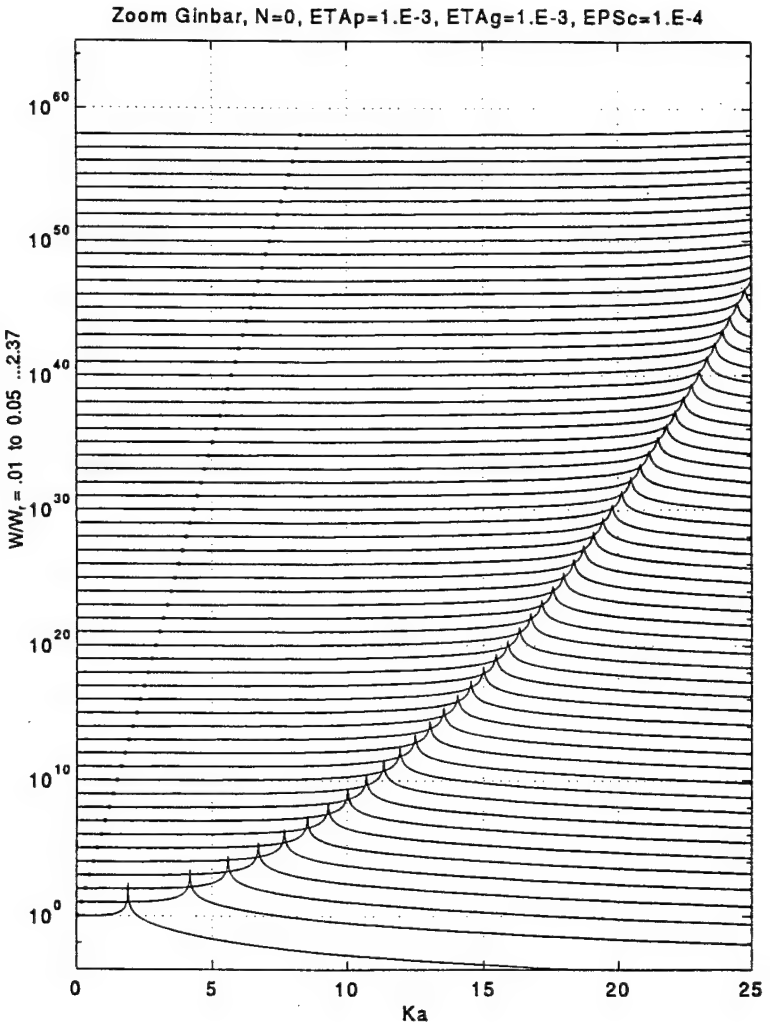

a. A hybrid cylinder; $\varepsilon_c = 10^{-4}$.

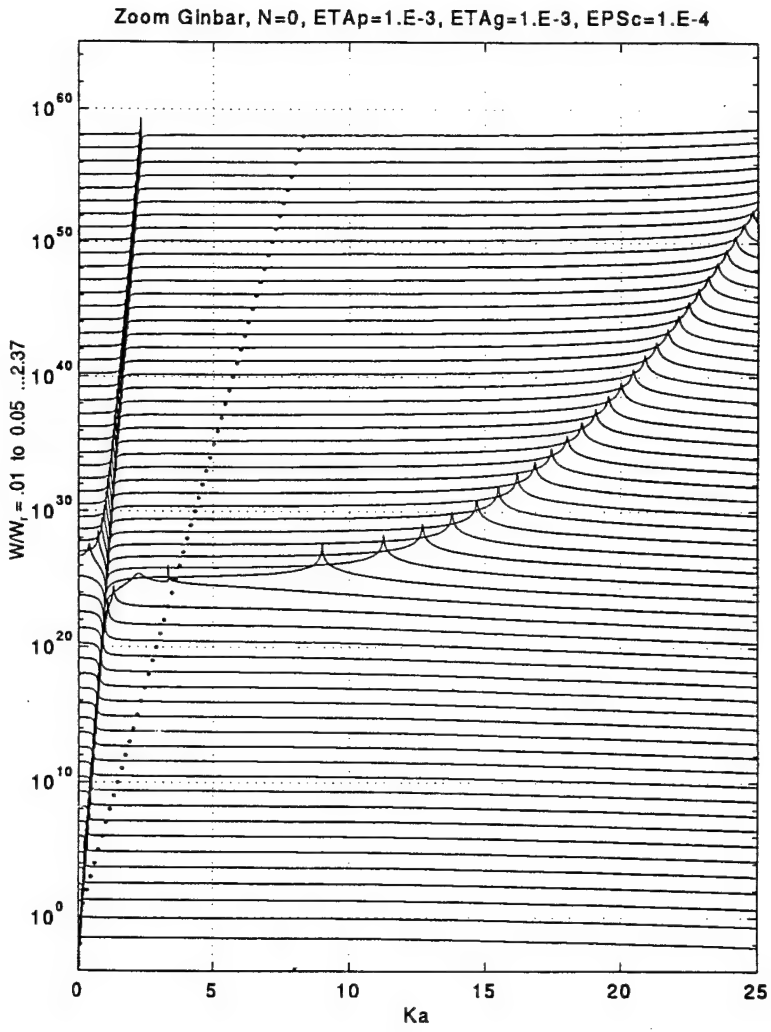

b1. A natural cylinder; $\varepsilon_c = 10^{-4}$.

Fig. 4. The normalized modal response $\overline{V}_{\infty n}(k,\omega)$ as a function of (ak) in a frequency waterfall format pertaining to the lower spectral range. Standard parametric values are used, except that the mode index (n) is zero and the fluid loading parameter (ε_c) is as specified. Superimposed is the sonic locus represented by discrete dots.

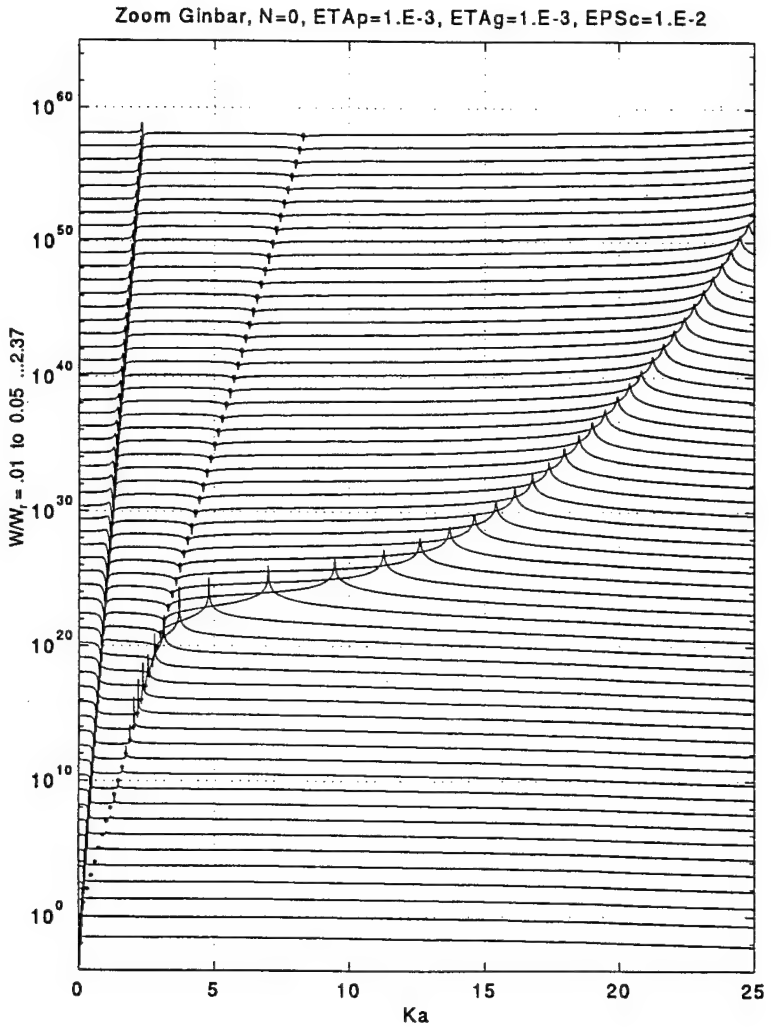

b2. $\varepsilon_c = 10^{-2}$.

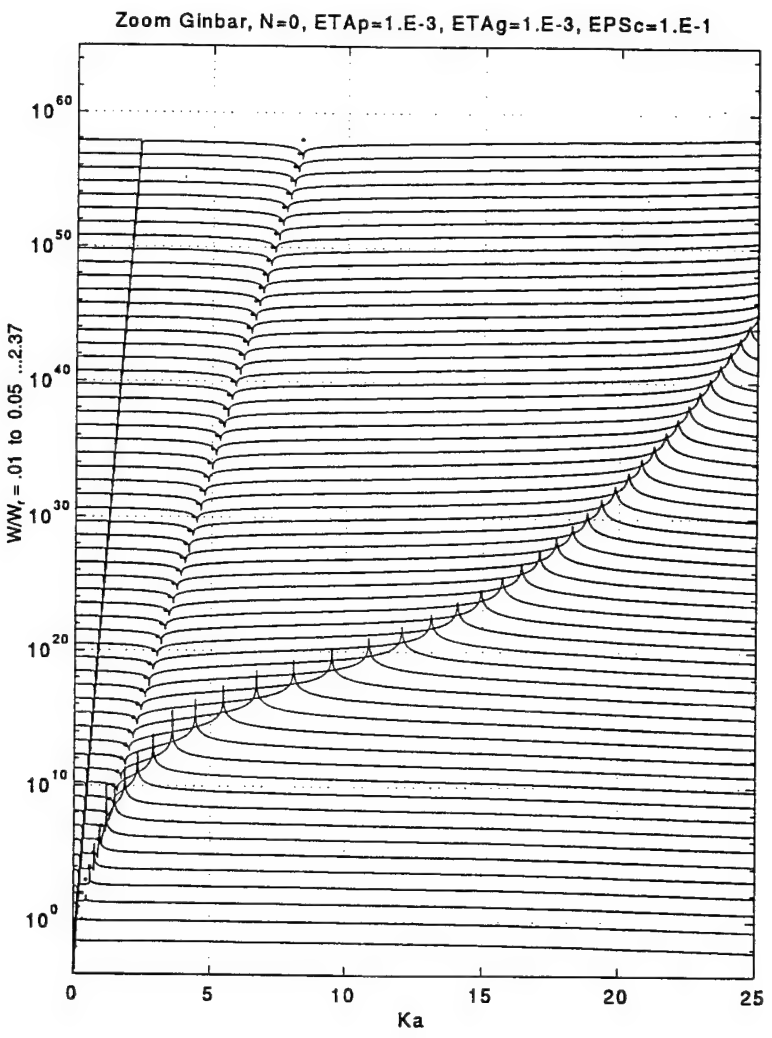

b3. $\varepsilon_c = 10^{-1}$.

Fig. 4. Continued

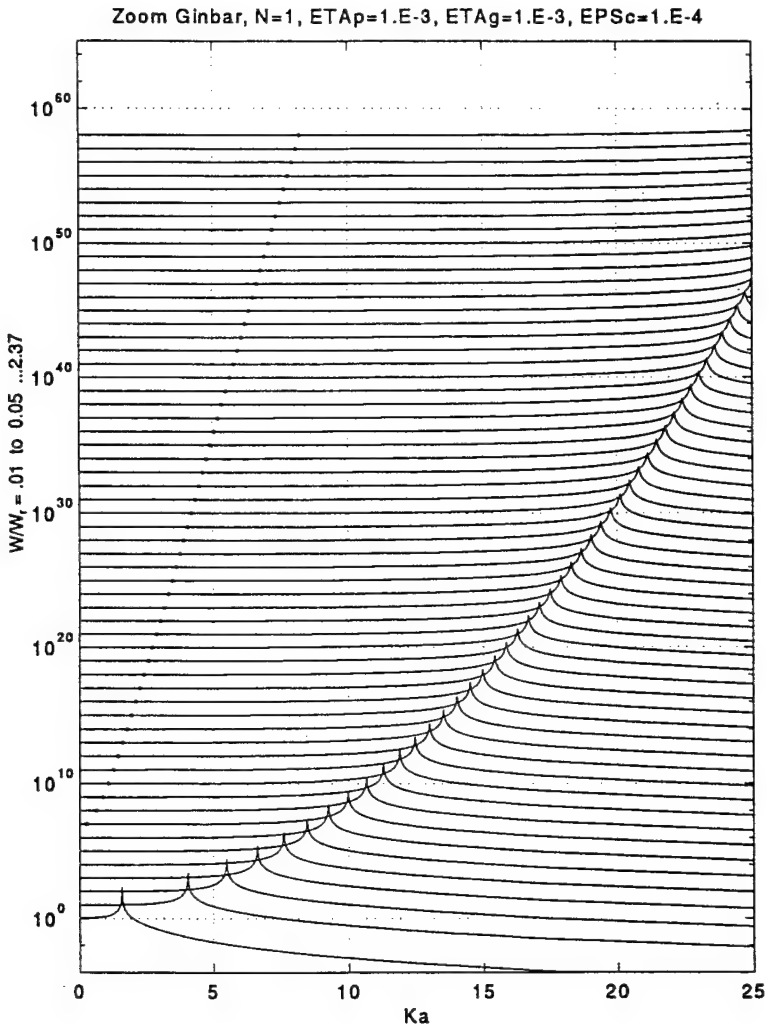

a. A hybrid cylinder; $\varepsilon_c = 10^{-4}$.

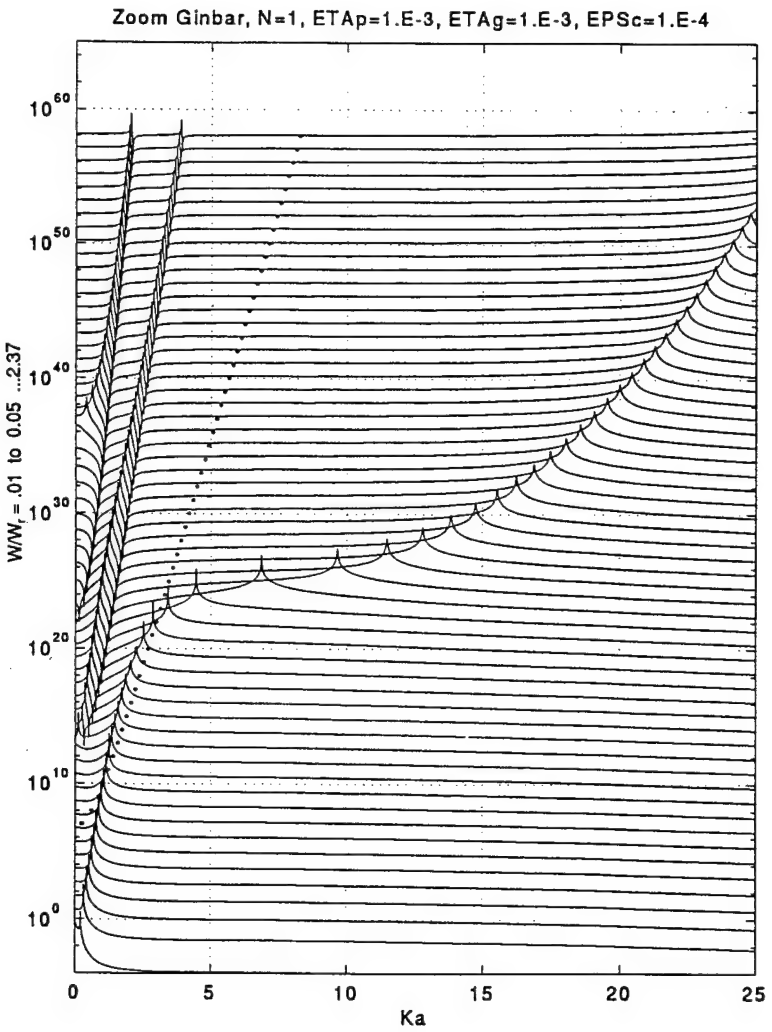

b1. A natural cylinder; $\varepsilon_c = 10^{-4}$.

Fig. 5. As Fig. 4 except that the mode index (n) is unity.

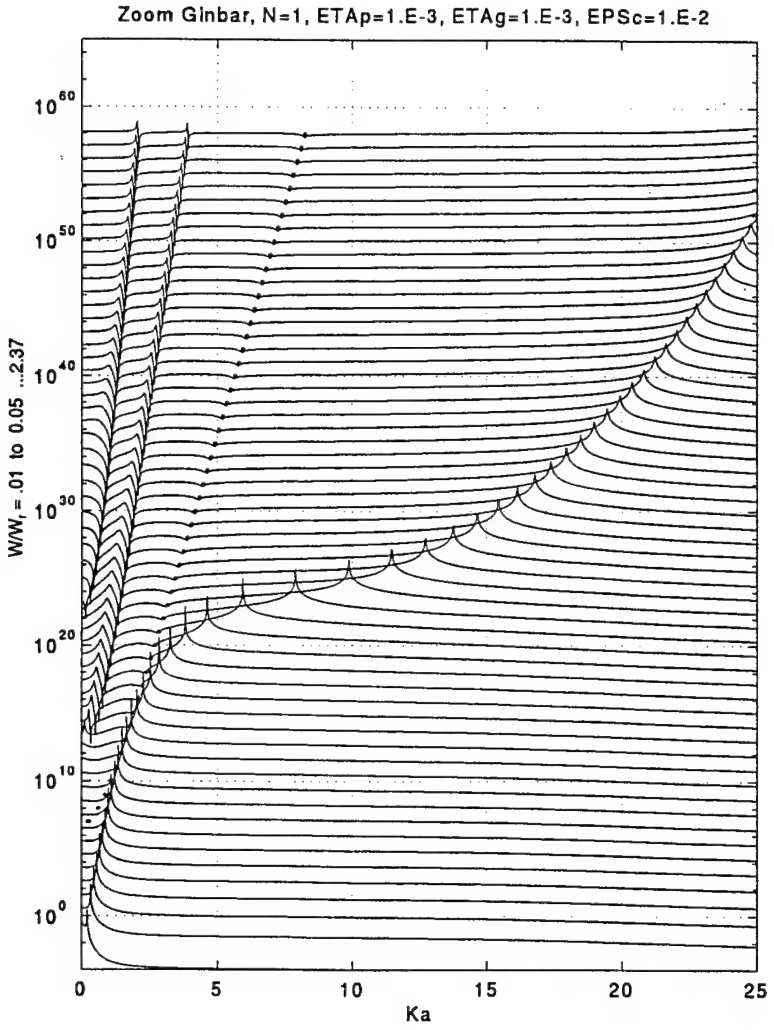

b2. $\varepsilon_c = 10^{-2}$.

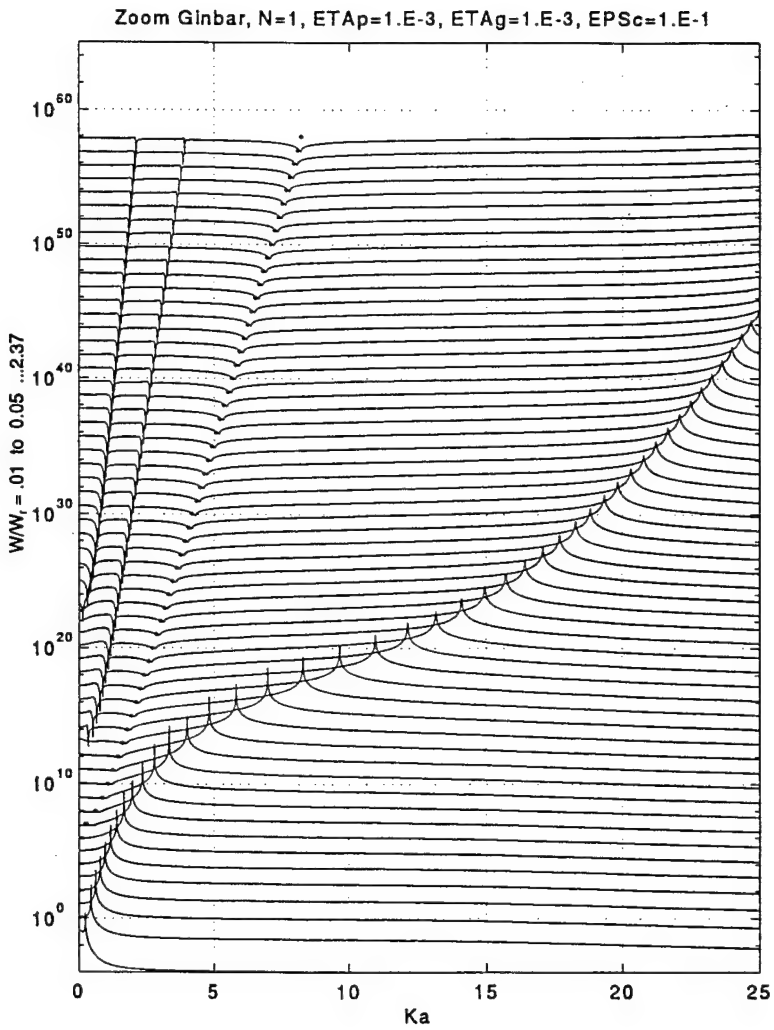

b3. $\varepsilon_c = 10^{-1}$.

Fig. 5. Continued

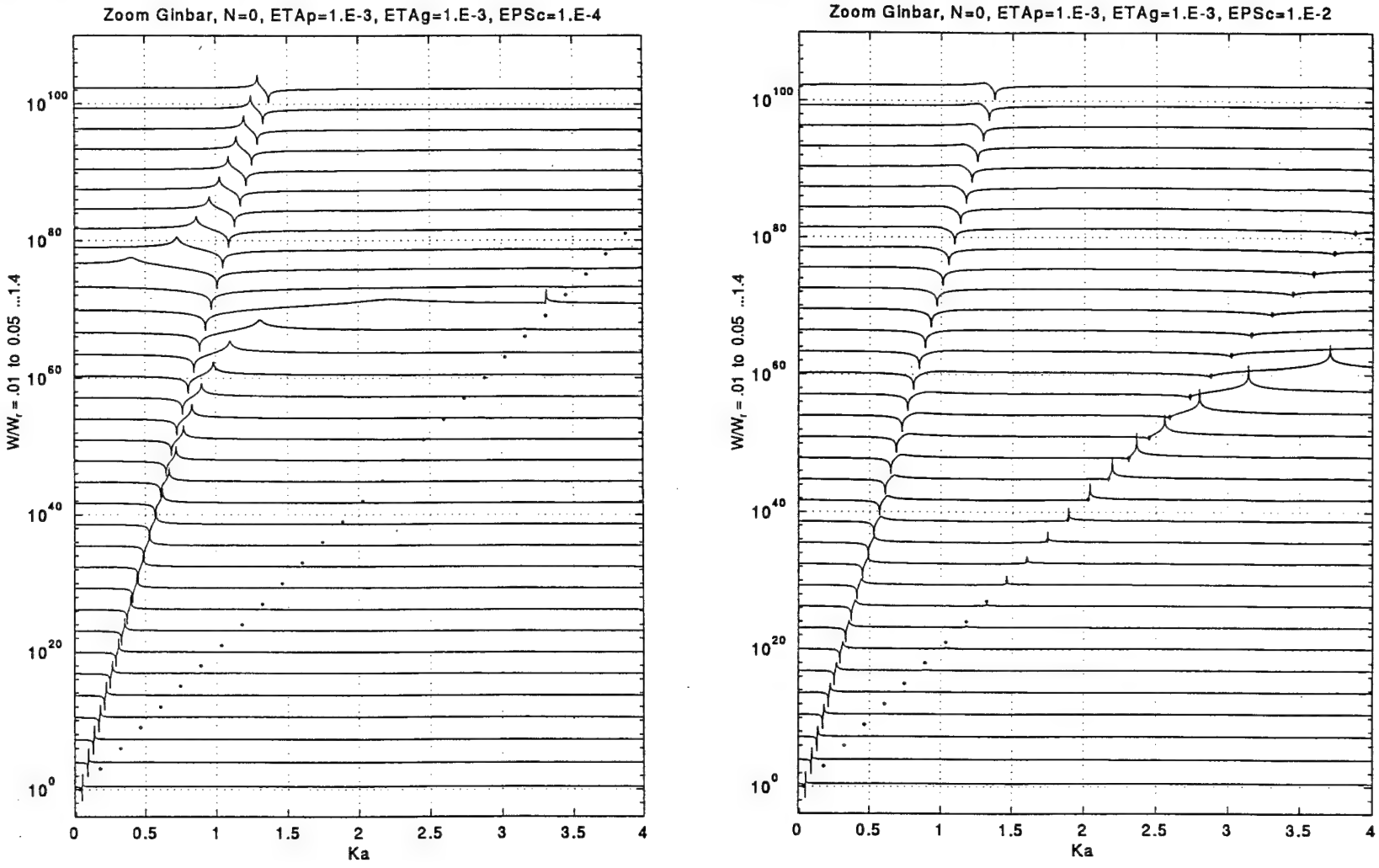

a. $\varepsilon_c = 10^{-4}$.

b. $\varepsilon_c = 10^{-2}$.

Fig. 6. The normalized modal response $\overline{V}_{\infty n}(k, \omega)$ as a function of (ak) in a frequency waterfall format pertaining to the zoom on region in the lower spectral range. Standard parametric values are used, except that the mode index (n) is zero and the fluid loading parameter (ε_c) is as specified. Superimposed is the sonic locus represented by discrete dots.

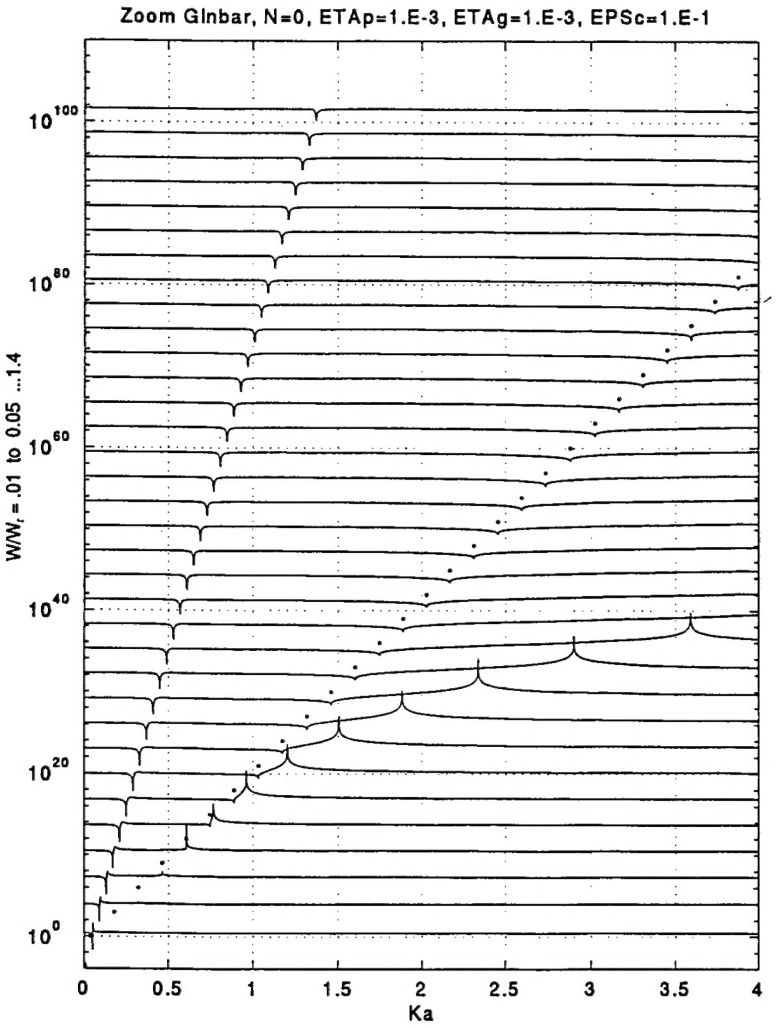

c. $\varepsilon_c = 10^{-1}$.

Fig. 6. Continued.

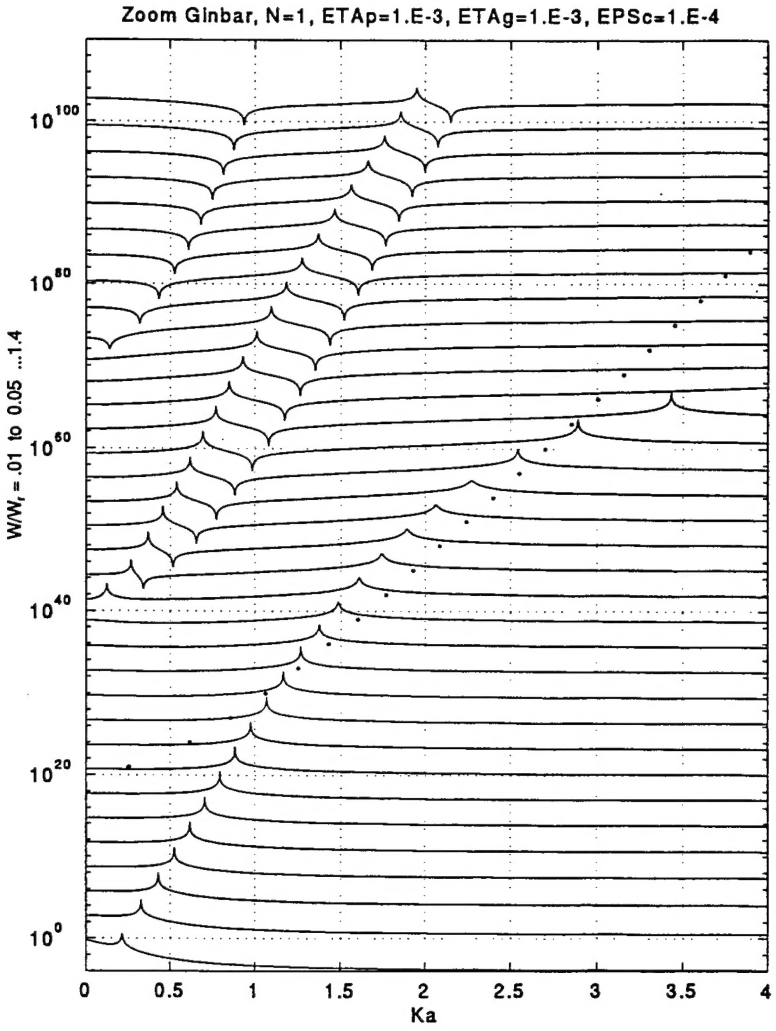

a. $\varepsilon_c = 10^{-4}$.

Fig. 7. As Fig. 6 except that the mode index (n) is unity.

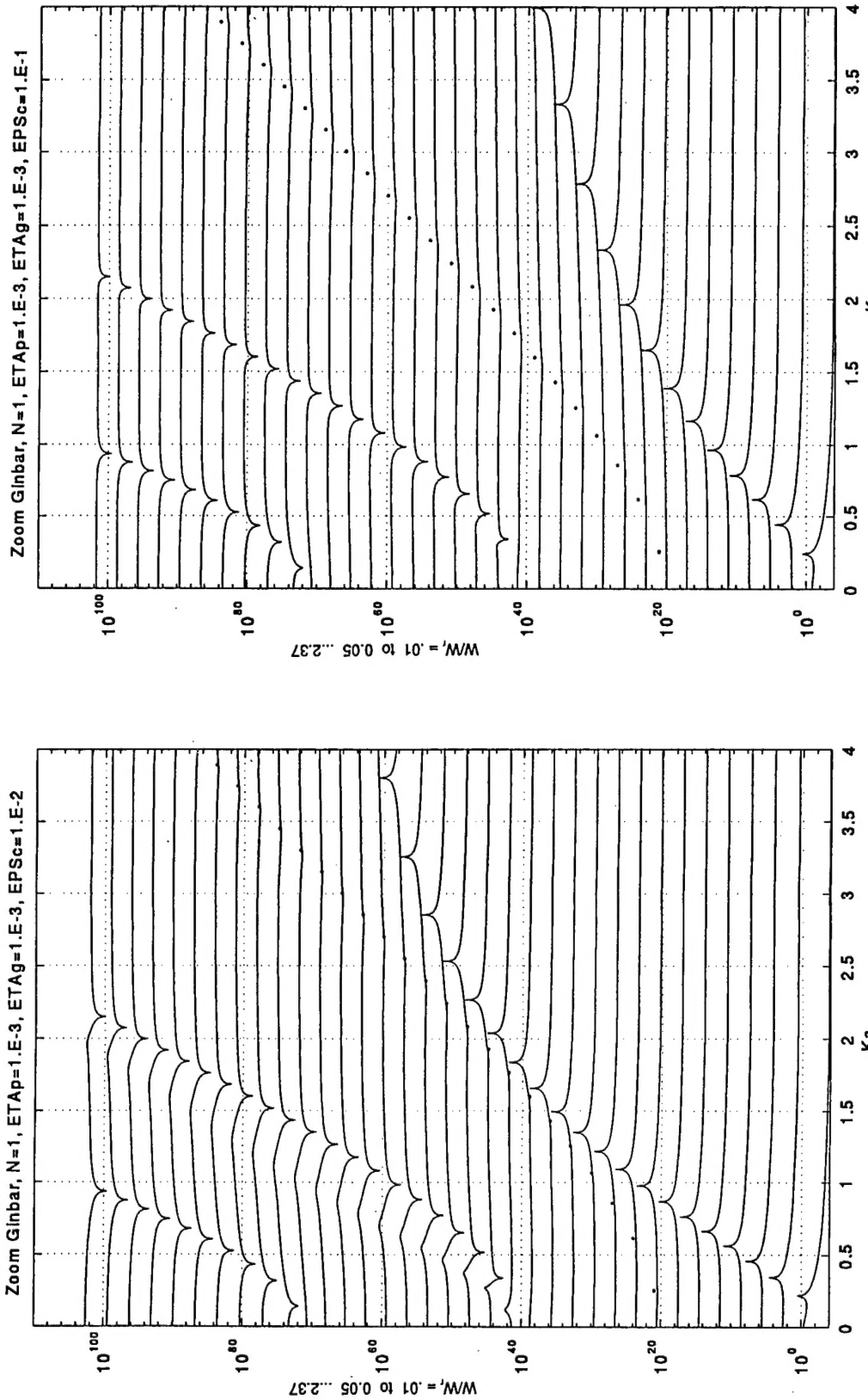

b. $\varepsilon_c = 10^{-2}$.

c. $\varepsilon_c = 10^{-1}$.

Fig. 7. Continued

REFERENCES

1. G. Maidanik and K.J. Becker, "Phenomena of aliasing and pass and stop bands in the drive in lieu of ribs on cylindrical shells," NSWCCD report no. SIG-96/072-7030 (1996).
2. G. Maidanik and K.J. Becker, "Computation of the Modal Response of Regularly Ribbed Cylinders," soon to be published in the J. Acoust. Soc. Am. (1997).
3. J. Dickey, G. Maidanik and H. Überall, " The splitting of dispersion curves for the fluid loaded plate," J. Acoust. Soc. Am., 98, 2365-2367 (1995).
4. D. G. Crighton, "The green function of an infinite, fluid loaded membrane," J. Sound Vib. 86, 411-433 (1983)," and "Transmission of energy down periodically ribbed elastic structures under fluid-loading," Proc. R. Soc. London A394, 405-436 (1984).
5. D.M. Photiadis, "The propagation of axisymmetric waves on a fluid-loaded cylindrical shell," J. Acoust. Soc. Am. 88, 239-250 (1990), and J.F.M. Scott, "The free modes of vibration of an infinite fluid-loaded cylindrical shell," J. Sound Vib. 125, 241 (1988).
6. F. Fahy, Sound and Structural Vibration (Radiation, Transmission and Response), (Academic Press, 1985).
7. G. Maidanik and J. Dickey, "Velocity distributions on unloaded finitely and regularly ribbed membranes," J. Acoust. Soc. Am., 149, 43-70 (1991) and "Response of regularly ribbed fluid loaded panels," J. Acoust. Soc. Am., 155, 481-495 (1992).

INITIAL DISTRIBUTION

Copies		
3	NAVSEA 03T2	
	2	Taddeo
	1	Becker
4	ONR/ONT	
	1	334 Vogelsong
	1	334 Tucker
	1	334 Main
	1	Library
4	NRL	
	1	5130 Bucaro
	1	5130 Williams
	1	5130 Photiadis
	1	Library
4	NUWC/New London	
	1	Sandman
	1	Harari
	1	3332 Lee
	1	Library
1	NUWC/NPT Library	
2	DTIC	
2	Johns Hopkins University	
	1	Green
	1	Dickey
1	Applied Physics Lab Johns Hopkins University Library	
4	ARL/Penn State University	
	1	Biancardi
	3	Burroughs
1	Georgia Tech/M.E. Dept. Ginsberg	

Copies		
2	MIT	
	1	Dyer
	1	Manning
1	Penn State University	
	1	Koopman
2	Virginia Tech	
	1	Knight
	1	Fuller

CENTER DISTRIBUTION

Copies	Code	Name
1	011	
1	0112	Douglas
1	0112	Halsall
1	20	
1	204	
1	2040	Everstine
1	2042	
1	2042	Hambric
1	70	
1	7030	
1	7200	Hwang
1	7250	
1	7250	Maga
1	7250	Vasudevan
1	726	Szilagyi
2	3421	(TIC-Carderock)